



OPEN

Tracking mangrove restoration using a biogeochemical soil health index and ecosystem service indicators

Laís Coutinho Zayas Jimenez^{1,2}, Hermano Melo Queiroz^{3,4}✉, Maurício Roberto Cherubin^{1,4}, Francisco Ruiz¹ & Tiago Osório Ferreira^{1,4}✉

Mangrove forests provide critical soil-related ecosystem services (ES), including carbon sequestration, contaminant retention, and nutrient cycling—all closely linked to soil health. However, land-use change and pollution increasingly threaten mangrove soils, compromising their functionality and ES provision. To reverse these impacts, effective strategies must begin with robust assessments of soil health using key indicators that also reflect ecosystem functions. Despite their importance, soil health indexing methods for mangroves remain underdeveloped. This study proposes a soil health index (SHI) for mangrove ecosystems, applied in northeastern Brazil across degraded, restoring (9 and 13 years), and mature forests. We assessed variables linked to biogeochemical processes governing carbon dynamics (soil texture, soil organic carbon - SOC, pseudo-total Fe), contaminant immobilization (exchangeable, carbonate-bound, oxyhydroxide-bound, and pyritic Fe, redox potential, and pH), and nutrient cycling (β -glucosidase, acid phosphatase, and available phosphorus). SHI was constructed using a minimal dataset selected via principal component analysis. Mature mangroves showed the highest SHI values (0.99 ± 0.03), while degraded sites had the lowest (0.25 ± 0.01). Replanted areas displayed intermediate SHI values (0.37 ± 0.01 at 9 years; 0.52 ± 0.02 at 13 years), indicating gradual recovery. ES provision estimates followed the same trend. The SHI effectively captured soil health changes across degradation and restoration gradients and is a promising tool to inform decision-makers, support conservation planning, and communicate complex data in accessible formats. This approach strengthens links between science, restoration action, and ecosystem service outcomes.

Keywords Blue carbon, Contaminants sink, Nutrient cycling, Coastal ecosystems management, Mangrove restoration

Soil health is the capacity of soil to function as a living system that sustains plants, animals and humans and links soil science to decision-making¹. In mangroves, soil health denotes the ability of geochemically unique soils to maintain below-ground processes such as long-term organic-carbon retention, efficient nutrient cycling and geochemical attenuation of contaminants^{2,3}. Because these functions occur under waterlogged, redox-dynamic conditions, informative indicators must be sensitive to the geochemical environment in these soils, in addition to conventional physical and chemical attributes⁴⁻⁶. However, to date, most soil health indexes (SHI) were designed for well-aerated agricultural soils and therefore underrepresent these controls in blue carbon ecosystems, particularly mangroves. Globally, studies explicitly addressing soil health in mangrove ecosystems remain scarce. A recent review of over 8,000 mangrove soil papers found only about 4% addressing SH and fewer than 40 linking it to ecosystem services⁷. Research is concentrated mainly in India and Southeast Asia, where efforts focus on coastal soil degradation, microbial community dynamics, and plant-microbe interactions that support soil functionality under saline conditions^{8,9}. Other works examine land-use conversion effects, such as mangrove-to-paddy transformations, on microbial and enzymatic indicators^{10,11}. However, most studies

¹Luiz de Queiroz College of Agriculture, University of São Paulo (ESALQ-USP), Av. Pádua Dias 11, Piracicaba, São Paulo 13418-900, Brazil. ²Fundação para Conservação Produção Florestal do Estado São Paulo, Av. Prof. Frederico Hermann Júnior, 345, São Paulo 05459-010, SP, Brazil. ³Department of Geography, University of São Paulo, Av. Prof. Lineu Prestes, 338, Cidade Universitária, São Paulo 05508-900, SP, Brazil. ⁴Center for Carbon Research in Tropical Agriculture (CCARBON), University of São Paulo, Piracicaba 13418-900, Brazil. ✉email: hermanomelo@usp.br; toferreira@usp.br

emphasize isolated attributes rather than integrative soil health frameworks. No studies to date have assessed soil health in mangrove ecosystems in Brazil, underscoring a significant regional knowledge gap and the need for tailored approaches to these geochemically unique soils that may be useful for conservation or restoration actions.

Restoration of Blue Carbon ecosystems is widely promoted as a Natural Climate Solution (NCS) because these coastal wetlands store large quantities of organic carbon, primarily within their soils^{12–15}. In mangroves, soil-carbon accumulation reflects high primary production and tidal trapping of sediments together with hydrological and geochemical constraints on decomposition^{5,16–18}. Prolonged waterlogging limits O₂ diffusion and shifts microbial metabolism toward dissimilatory iron and sulfate reduction, pathways with lower energy yield than aerobic respiration that slow mineralization and favor organic-matter retention^{19–21}. These pathways have lower energy yield than aerobic respiration, slow mineralization and favor the retention of organic matter within the soil profile^{22,23}. As a result, soils commonly account for ~ 50–90% of total ecosystem carbon in mangroves, with stocks that can match or exceed those reported for many boreal and tropical forests^{24,25}. Additionally, end-products of iron and sulfate reduction also influence nutrient cycling and promote iron sulfide formation (e.g., pyrite) that can immobilize trace metals^{6,26–28}.

Despite this functional importance, large areas of tropical and subtropical shorelines have lost, or degraded mangrove cover mainly due to aquaculture, urban expansion and agriculture^{29–32}. In this context, management needs to both expand reforestation and evaluate ecosystem services through explicit identification and quantification. Evidence indicates that reforestation can contribute to the recovery of several services—coastal protection from flooding and storms, provision of nursery habitat and erosion control—yet the extent to which restoration and rehabilitation re-establish soil functions, and the regulating services that depend on them, remains insufficiently quantified^{4,33–35}. The outcomes are sensitive to site conditions and management choices, reinforcing the need for soil-based diagnostics to support local decisions.

Multivariate soil-quality indices derived from principal component analysis (PCA) or related approaches compress multiple measurements into a single score that can be tracked across sites and time³⁶. While such indices are established in agriculture, direct transfer to mangroves is limited because standard formulations omit variables that are central to tidally flooded soils (e.g., Eh, iron geochemistry) responsive to anoxia and salinity. A recent adaptation of an agricultural framework to young mangrove plantings demonstrated that a composite index is feasible but did not include these redox-sensitive variables and did not evaluate predictive relationships with specific services². Consequently, there is a methodological gap between the recognized need to monitor soil-based drivers of Blue Carbon and the tools used to guide restoration practice.

In recent years, advances in environmental monitoring and restoration assessment tools have expanded the ability to evaluate mangrove condition through vegetation and landscape indicators^{37–40}. However, approaches capable of quantifying belowground functionality remain scarce, even though soils regulate most of the biogeochemical processes that sustain ecosystem services^{2,3}. Developing indices that translate soil processes into practical measures is therefore essential to complement existing monitoring tools and improve restoration diagnostics⁴¹. Here we address this gap by assessing soil-health recovery with variables related to the biogeochemical control of carbon, inorganic contaminants and nutrients, and by evaluating a soil-health index tailored to mangroves as a decision-support metric. We test the hypothesis that provision of key services—carbon sequestration and contaminant immobilization and nutrient cycling — is positively associated with soil health, and that mangrove restoration can shift soils along this trajectory. Specifically, we assembled a variable set that includes geochemical data alongside conventional physical and chemical properties to construct a composite index using PCA across a 9–13-year restoration chronosequence in an estuarine setting in Northeast Brazil.

Materials and methods

Study site description and soil sampling

The study was conducted in the Cocó River estuary (3°46'25.04" S; 38°26'9.66" W), located in the state of Ceará, in Brazil's Northeast region. The study area is subjected to a semi-arid climate with influences from the Intertropical Convergence Zone, characterizing a seasonal distribution of rainfall (i.e., a dry period from June to December and a rainy period from January to May). The average annual precipitation is less than 900 mm, and the average annual temperature is 27 °C. Additionally, the region is characterized by the predominance of trade winds from the northeast and southeast. The estuary experiences a diurnal tidal regime with tide amplitudes ranging from 0.75 to 3.25 m. Moreover, the coastal morpho dynamics in the region has a greater tendency to erosion and are predominantly modified by the tides, wind direction and intensity, and waves moving in N and NNE directions which can cause local erosive events that results in damage to the urban buildings^{42,43}.

The coastal zone of the region is classified as a straight, sandy coast with dunes, lagoons, and salt flats. These features originated from the Barreiras Formation, which is mainly composed of sedimentary rocks from the Tertiary-Quaternary period⁴³. In the Cocó River estuary (Fig. 1), the presence of beach sandstones of fluvio-marine origin is also observed, cemented by the precipitation of calcium carbonate due to differences in freshwater and saltwater saturation⁴⁴.

Undisturbed soil samples were collected in 2021, from mangrove areas with different ages of replanting (9 and 13 years old), which were compared to adjacent mature and degraded mangroves (Fig. 1). The selection of soil sampling locations was based on the area's historical context and land-use trajectory. This ensured that each scenario (degraded, restoring for 9 and 13 years old, and mature forests) represented a distinct ecological and restoration stage. The region was previously deforested and degraded mostly due to urban expansion. However, since 2006, the Cocó River estuary has been designated as a conservation area under the Environmental Protection Area of Sabiaguaba, initiating reforestation efforts. Despite the creation of the protection area, the region is marked by the process of coastal zone artificialization due to urbanization in the surrounding areas, leading to severe consequences for sedimentary balance⁴³. There is a horizontal and low verticalization that is



Fig. 1. Overview of the study area in the Cocó River estuary, Ceará, Northeast Brazil. The figure illustrates the locations of the 9- and 13-years-old replanted mangroves compared to degraded and pristine mangroves. The satellite images point out the transformation over time, emphasizing the differences between the 9-year-old and 13-year-old areas in 2014 (six years after the replanting began) and 2023. The x and y axes represent geographical coordinates. Images © 2024 Google Earth, © Google Maps.

not planned, surrounding the region with a set of family residences or developments consisting of houses and apartments⁴⁵.

The mangrove reforestation activities were a collaborative effort involving public and private initiatives, coordinated by NGOs, and carried out by volunteers. Their main objectives included environmental education, ecosystem restoration, and support for local ecotourism. Seedlings were prepared from locally collected propagules and then transplanted to designated areas for reforestation.

The classification of mangrove sites into degraded, replanted (with 9- and 13-years-old), and mature was based on vegetation structure, land-use history, and degree of ecological recovery. All plots were located within the Sabiaguaba Environmental Protection Area, approximately 100 m apart from one another. The mature mangrove represents a well-developed forest, undisturbed for at least three decades, covering about 13,000 m² and composed mainly of *Avicennia germinans* (L.) L., *Laguncularia racemosa* (L.) C.F., and *Rhizophora mangle* L. The replanted sites, aged 9 and 13 years, were established through community-based initiatives using *Rhizophora mangle* L. propagules in previously deforested areas. These areas, measuring approximately 3,500 and 1,000 m², respectively, exhibit developing canopy structure, partial litter cover, and improved hydrological connectivity compared to the degraded zone. The degraded mangrove, covering roughly 1,000 m², lacks vegetation due to prior deforestation and hydrological alteration.

The soil sampling was carried out during low tide in each mangrove scenario using short transects of approximately 40 m, with one sample taken every 10 m, totaling four samples per scenario. The soil collection was performed using polyvinyl chloride (PVC) tubes (50 mm in diameter and 50 cm in height), prewashed with 10% HCl, and attached to a stainless-steel auger specifically designed for waterlogged soils^{46–48}. The PVC tubes were carefully inserted into the soil to obtain intact cores and then hermetically sealed to prevent chemical or biological alterations. Samples were transported vertically in thermal boxes at approximately 4 °C to the laboratory, following standard procedures for carbon quantification in coastal environments.

In the laboratory, each soil core was sectioned into four depth intervals: 0–10, 10–20, 20–30, and 30–40 cm. These subsamples were therefore treated as replicates, and their values were averaged to represent the overall condition of each sampling site.

Determination of soil parameters (indicators) for health index

The soil pH and Eh values were acquired in situ using portable meters (HANNA, model HI98121, Hanna Instruments, Woonsocket, RI, USA). The pH meter featured a glass electrode and was calibrated beforehand with standard solutions (pH values of 4 and 7). Eh values were determined using a platinum electrode previously validated with a control solution (HI7021M 240 mV, 25 °C, ORP test solution).

Undisturbed soil cores, collected with minimal compaction, were employed for soil bulk density (BD) determination. The cores were weighed wet and then dried at 60 °C until a constant weight was achieved, a procedure used to avoid organic matter loss. Soil BD was calculated using the mass of oven-dried soil solids and the total soil volume (depth and tube diameter).

In the laboratory, soil organic carbon (SOC) was quantified using a Flash Elemental analyzer (Thermo Fisher Flash HT 2000; Thermo Scientific™) coupled to a Thermo Fisher Delta V (Thermo Scientific™). For SOC determination, collected samples were previously acidified with 1 mol L⁻¹ HCl to eliminate carbonates²⁵. Subsequently, samples were dried at 45 °C until a constant weight was attained and then weighed for SOC determination. The soil carbon stocks (SCS) were determined from SOC using the equation $SCS = \sum SOC_i \times BD_i \times \text{thickness of the layer } (i)$, using values of BD, SOC, and the thickness of each analyzed soil layer in the studied areas²⁵.

A sequential iron extraction method, integrating techniques proposed by Tessier, Campbell, and Bisson⁴⁹, Huerta-Diaz and Morse⁵⁰, and Fortín et al.⁵¹, was employed for the determination of six operationally distinct fractions (Table 1). For the sequential iron analysis, sub-samples were collected from the central part of the moist samples, avoiding the use of external portions exposed to the atmosphere, which may have oxidized free forms of iron⁵². This approach facilitates the calculation of the degree of pyritization (DOP), determining the percentage of iron in the FeEX, FeCA, FeFR, FeLP, and FeCR fractions (Table 1) incorporated into the pyritic fraction in relation to the pseudo-total iron (pseudo-total Fe), represented by the sum of the six determined fractions⁵³. The extraction solutions sequentially from FeEX to FeCR fractions were pre-purged with N₂ flow under heating to remove oxygen and prevent the oxidation of reduced forms of iron and sulfur⁵². Furthermore, iron content in each extract was quantified using inductively coupled plasma - optical emission spectrometry, and reference standard solutions were employed, with iron concentrations recovered exceeding 90%.

Fraction	Abbreviation	Extracting solution
Exchangeable iron	FeEX	MgCl ₂ 1 mol L ⁻¹ (pH 7.0)
Carbonate-associated iron	FeCA	NaOAc 1 mol L ⁻¹ (pH 5.0)
Ferrihydrite-associated iron	FeFR	Hydroxylamine 0.04 mol L ⁻¹ + acetic acid 25% at 30 °C
Lepidocrocite-associated iron	FeLP	Hydroxylamine 0.04 mol L ⁻¹ + acetic acid 25% at 96 °C
Hematite and goethite-associated iron	FeCR	20 ml sodium citrate 0.25 mol L ⁻¹ + sodium bicarbonate 0.11 mol L ⁻¹ with 3 g sodium dithionite at 75 °C
Pyritic iron	FePY	Concentrated HNO ₃ after pretreatment with concentrated H ₂ SO ₄ and 10 mol L ⁻¹ HF

Table 1. Description of the iron fractionation analysis according to Tessier et al.⁴⁹, Huerta-Diaz and Morse⁵⁰, and Fortin et al.⁵¹.

Soil particle size distribution (i.e., sand, silt, and clay contents) was determined using the pipette method⁵⁴ after pretreatment with hydrogen peroxide (30% solution) to remove soil organic carbon, followed by mechanical (agitation for 12 h) and chemical dispersions (0.15 mol L⁻¹ sodium hexametaphosphate and 1 mol L⁻¹ sodium hydroxide).

Available phosphorus (available-P) was determined through extraction with Mehlich-3⁵⁵, and its concentration was quantified by colorimetry at 880 nm. Acid phosphatase was determined according to the method of Tabatabai and Bremner⁵⁶, using (p)-nitrophenyl phosphate as a substrate and reported as $\mu\text{g p-nitrophenol produced g}^{-1}$ soil h⁻¹. β -Glucosidase activity was estimated using mM p-nitrophenol- β -D-glucopyranoside as the substrate⁵⁷.

The selected analytical parameters consider the determination of physicochemical factors that characterize the environment and its geochemical functioning, such as redox conditions, metabolic pathways for iron and sulfate reduction, contaminant immobilization, nutrient cycling, and carbon accumulation capacity.

Determination of soil health index (SHI)

The SHI was determined following the procedure adopted by Faridah-Hanum et al.⁴¹, where a minimal set of data was selected through multivariate analyses. Principal Component Analysis (PCA) was utilized to select appropriate indicators and as a method to extract weighting factors^{58–60}. For interpretation, two principal components explaining over 50% of the data variance were employed. Furthermore, only factors with eigenvalues ≥ 1.0 in at least 5% of the data variation were considered^{58,59}. The retained factors were then subjected to varimax rotation, a statistical procedure to simplify the data structure by clarifying the relationship between variables and factors⁶¹. This rotation enhances interpretability by making each variable more strongly associated with one specific factor. In each principal component, the selected variables were those for which the factor with the highest squared cosine was obtained. The rotated factor loadings (see Supplementary Material) of the selected attributes were used in calculating the relative weights of attributes in the SHI, as per the equation:

$$W_i = \frac{F_{1i}P_{1i} + F_{2i}P_{2i}}{(\sum_{j=1}^n F_{1j}P_{1j}) + (\sum_{j=1}^n F_{2j}P_{2j})} \quad (1)$$

where, W_i : relative weight of the attribute in the i -th variable composing the SHI; F_{1i} and F_{2i} : eigenvalues of the principal components; P_{1i} : rotated factor loading of the attribute in the i -th variable; P_{2i} : rotated factor loading of the attribute in the j -th variable; i and j : indices for variables; n : number of variables involved in the PCA.

After selecting the indicators, the values were normalized through relative standardization (linear transformation)⁶² to be included in the SHI, transforming them into indicator scores (S_i) ranging from 0 to 1^{63,64}. The indicators were ranked in ascending or descending order, where the highest value could be considered detrimental or beneficial, respectively. For indicators assumed as “more is better,” each observation was divided by the highest observed value, with the highest value considered a score of 1. For indicators considered “less is better,” the lowest observed value (in the numerator) was divided by each observation (in the denominator), so that the lowest value received a score of 1. For those indicators where neither higher nor lower is better (“optimal”), observations were scored as “more is better” up to a limit (i.e., the highest observed value in the mature mangrove for the respective variable) and then scored as “less is better” when above this established limit⁶³. Thus, the SHI was determined by the equation:

$$\text{SHI} = \sum_{i=1}^n (W_i \times S_i) \quad (2)$$

where, SHI: is a number between 0 and 1; W_i : corresponding weight to the i -th parameter, a number between 0 and 1; and S_i : score of the i -th indicator defined using PCA results, a number between 0 and 1. In the model, higher indices indicate better soil quality or better soil function performance.

Estimate of ecosystem services provision

For representation of ecosystem services, specific soil attributes were used as proxies for climate regulation, nutrient cycling, and contaminant immobilization services. The SOC, pseudo-total Fe, and clay contents were chosen to represent organic carbon sequestration, reflecting Climate Regulation. The FeFR, FeLP, FeCR, and FePY content, were chosen to represent contaminant immobilization, as many contaminants, (e.g., heavy metals), can precipitate with pyrite and iron oxyhydroxides, thus turn into immobilized^{26,65,66}. Additionally, available P, and the enzymes acid phosphatase and β -glucosidase were chosen to represent nutrient cycling as they respond to the release and availability of phosphorus and microbial activity associated with the mineralization of nutrients derived from organic matter. These services represent ecosystem services related to regulation, such as carbon sequestration and contaminant immobilization, as well as support services, including nutrient cycling.

To estimate the ecosystem services, all data were initially normalized on a scale from 0 to 1. This normalization was done by linear transformation, adjusting the data based on the maximum values of the selected variables. Subsequently, the mean values of the normalized data for each scenario studied were calculated and then summed to represent the different ecosystem services for each scenario and further normalized on a scale from 0 to 1. After normalization, the values representing the ecosystem services were presented in a bar chart.

Statistical analysis

All statistical analyses were performed using XLSTAT software v.2014.5.03 at a 5% significance level ($p < 0.05$). The Shapiro–Wilk test was initially applied to assess the normality of the data. As most variables did not meet the assumptions of normal distribution, an expected outcome for environmental datasets, the Kruskal–Wallis

non-parametric test was employed to evaluate differences among the four mangrove conditions (degraded, 9- and 13-year-old reforested, and mature forests). When significant differences were detected, multiple pairwise comparisons were conducted using Dunn's test. In addition, variables selected for the PCA, described in Sect. 2.3, were subjected to Spearman's rank correlation analysis ($p < 0.05$) to identify associations among soil attributes and to support the construction of the SHI (Table S1). All figures were generated using SigmaPlot software v.11.0 and subsequently refined for color adjustments using Paint.NET v.5.1.9.

Results

Soil indicators in the degraded, replanted, and mature mangroves

The physicochemical parameters (i.e., pH and Eh) indicated the occurrence of suboxic conditions, with significant differences among sites (Table 2). The highest Eh values were observed in the 9-year-old mangrove ($p < 0.001$), while the degraded, 13-year-old, and mature stands did not show significant differences. Regarding pH, the highest values ($p = 0.007$) occurred in the 13-year-old and mature mangroves, followed by the 9-year-old site, with the lowest value recorded in the degraded area (Table 2).

Most iron fractions showed significant variation along the restoration gradient ($p < 0.001$; Table 2). Exchangeable Fe (FeEX) varied slightly ($p < 0.001$), whereas carbonate-associated Fe (FeCA) decreased markedly in the replanted stands before increasing again in the mature mangrove ($p = 0.0032$). Ferrihydrite- and lepidocrocite-associated pools (FeFR and FeLP) increased progressively with restoration age ($p < 0.001$ and $p = 0.0007$, respectively), each increasing nearly fourfold from degraded to mature soils. Crystalline Fe (FeCR) and pyritic Fe (FePY) also increased sharply toward mature conditions ($p < 0.001$), leading to significantly higher pseudo-total Fe and degree of pyritization (DOP) in the mature forest ($p < 0.001$; Table 2).

Soil organic carbon (SOC) and soil carbon stocks (SCS) increased significantly along the chronosequence ($p < 0.0001$ and $p = 0.0056$, respectively), evidencing rapid belowground carbon accumulation after replanting (Table 2). Textural fractions also differed among sites ($p < 0.0001$): clay and silt contents increased toward mature mangroves, while sand declined substantially. Available phosphorus rose modestly but significantly ($p = 0.0050$), and β -glucosidase activity followed a comparable pattern ($p = 0.0202$). Acid phosphatase did not differ significantly across sites ($p = 0.1530$).

Soil health index (SHI) indicators using PCA analysis

The PCA indicates that the two selected components account for 58% of the total data variance (eigenvalues PC1 and PC2: 8.6298 and 1.7765, respectively). PC1 is primarily composed of variables such as FeEX, FeFR, FeLP, FeCR, FePY, DOP, pseudo-total Fe, SOC, clay, silt, sand, and available P, explaining 48% of the data variance (Fig. 2A). PC2 comprises pH and β -glucosidase variables, explaining 10% of the data variance (Fig. 2A). Mature mangrove areas and the 13-years-old replanted area were more influenced by higher contents of FeEX, FeFR, FeLP, FeCR, FePY, DOP, pseudo-total Fe, SOC, SCS, clay, silt, pH, and available P, along with higher β -glucosidase activity and lower acid phosphatase activity (Fig. 2A). On the other hand, the degraded mangrove

Variable	Unit	Degraded	9-year-old	13-year-old	Mature
Eh	mV	179.7 ± 15.5a	109.0 ± 42.3b	179.8 ± 35a	156.3 ± 59.8a
pH		6.4 ± 0.8c	7.1 ± 0.2ab	7.2 ± 0.3a	7.1 ± 0.3a
FeEX		11.2 ± 1.1c	7.9 ± 3.7cb	15.5 ± 3.1ab	21 ± 6.4a
FeCA		71.6 ± 13.4a	43.2 ± 20.8b	35.8 ± 10b	60 ± 47.8ab
FeFR		174.1 ± 36.3c	358 ± 182.6bc	521.6 ± 246.8ab	718.6 ± 367.9a
FeLP	mg kg ⁻¹	694.4 ± 104.7b	1,665.8 ± 890.7b	2,017.5 ± 682.3a	1,812.2 ± 514b
FeCR		216.7 ± 48.7b	1,021.7 ± 759a	1,802.8 ± 667.1a	1,313 ± 342.7a
FePY		53.9 ± 27.4c	221.1 ± 130.7bc	534 ± 451.1b	5,375.2 ± 2465.4a
Pseudo-total Fe		1,235.4 ± 177.5c	3,234.5 ± 1768.7bc	5,072.3 ± 1,698.1b	9,042.8 ± 3256.2a
DOP	%	4.6 ± 1.8b	8.8 ± 8.3b	10.3 ± 7.2b	53.3 ± 19.6a
SOC		0.6 ± 0.1c	1.0 ± 0.6bc	2.1 ± 1.4ab	4.8 ± 2.5a
SCS	Mg C ha	44.5 ± 34.8b	77.7 ± 37.7ab	92.4 ± 29.3a	115.7 ± 61a
Clay		3.7 ± 1.0c	14.3 ± 7.5b	24.2 ± 8.3b	42 ± 5a
Silt	%	1.8 ± 1.2b	5.6 ± 4.6b	12.7 ± 8.9b	28.4 ± 4.9a
Sand		94.1 ± 1.3a	80.3 ± 11.7ab	63.4 ± 16.3b	28.8 ± 8.8c
Available P	mg kg ⁻¹	194.1 ± 48.8c	244.4 ± 70.9ab	303.4 ± 102.7a	318.4 ± 106.1a
β -glucosidase	$\mu\text{g PNP g}^{-1} \text{ soil h}^{-1}$	14.2 ± 3.8b	19.1 ± 2.5a	19.2 ± 3a	19.5 ± 4.4a
Acid phosphatase		145.9 ± 62.8b	198.3 ± 35.4a	209.4 ± 55.8a	189.6 ± 35.6a

Table 2. Soil variables assessed in the replanted mangroves compared to the mature and degraded mangroves. Different lowercase letters indicate significant differences according to the Kruskal-Wallis test followed by Dunn's post-hoc comparison at $p < 0.05$. Eh: redox potential; FeEX: exchangeable iron; FeCA: carbonate-associated iron; FeFR: ferrihydrite-associated iron; FeLP: lepidocrocite-associated iron; FeCR: hematite and goethite-associated iron; FePY: pyritic iron; DOP: degree of iron pyritization; SOC: soil organic carbon; SCS: soil carbon stocks.

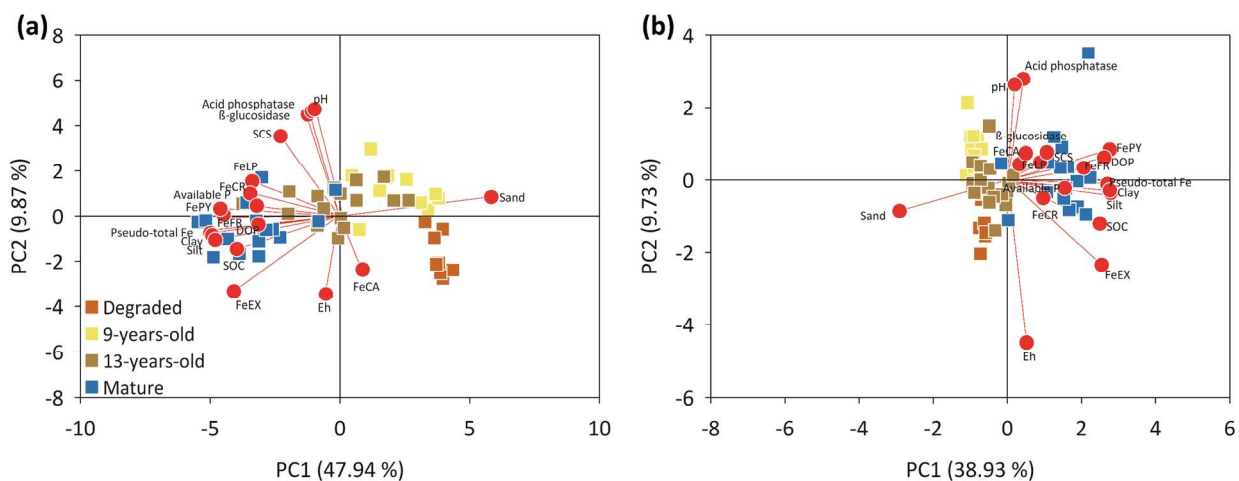


Fig. 2. (A) Principal component analysis (PCA) results for soil variables in degraded, 9-years-old replanted, 13-years-old replanted, and mature mangrove areas. (B) The PCA results submitted to varimax rotation to appropriately select variables composing the SHI. Eh: redox potential; FeEX: exchangeable iron; FeCA: carbonate-associated iron; FeFR: ferrihydrite-associated iron; FeLP: lepidocrocite-associated iron; FeCR: hematite and goethite-associated iron; FePY: pyritic iron; DOP: degree of iron pyritization; SOC: soil organic carbon; SCS: soil carbon stocks.

was more strongly influenced by higher Eh values and FeCA and sand contents, while the 9-years-old replanted area was influenced by lower Eh values and FeCA content (Fig. 2B).

After varimax rotation, PC1 accounted for 39% of the total data variance, while PC2 accounted for 10%, explaining a total of 47% of the variation (Fig. 2B). Thus, the variables selected as indicators for the SHI are those composing PC1, including FeEX, FeFR, FePY, DOP, pseudo-total Fe, SOC, clay, silt, sand, and available P (squared cosines: 0.664, 0.438, 0.779, 0.698, 0.744, 0.638, 0.792, 0.781, 0.808, and 0.251, respectively), and those composing the PC2 which includes Eh, pH, and acid phosphatase (squared cosines: 0.521, 0.388, and 0.356, respectively).

Among the selected variables, FePY, sand, clay, silt, FeEX, DOP, pseudo-total Fe, and SOC had higher weights (0.103, 0.100, 0.098, 0.098, 0.097, 0.097, 0.097, and 0.090, respectively), while FeFR, available P, Eh, pH, and acid phosphatase had weights of 0.076, 0.056, 0.036, 0.030, and 0.022, respectively (Fig. 3). The SHI revealed a clear gradient of ecosystem functioning across the mangrove conditions. Soils in the mature mangrove displayed the highest SHI values (0.99 ± 0.03 ; p -value < 0.001), indicating near-optimal functioning (Fig. 3). In contrast, degraded mangrove soils exhibited the lowest values (0.25 ± 0.01), functioning at only a quarter of their potential. Restoration efforts showed a positive effect on soil health, with improvements depending on the time since replanting (Fig. 3). After 9 years of restoration, soil functioning reached 37% of its potential ($\text{SHI} = 0.37 \pm 0.01$), showing no significant difference from the degraded site. However, after 13 years, restored soils reached 52% of their capacity ($\text{SHI} = 0.52 \pm 0.02$), significantly higher than the degraded area and approaching values observed in mature mangroves (Fig. 3). These results underscore the gradual recovery of soil functioning through restoration, though long-term efforts are needed to achieve full ecosystem recovery.

Estimate of ecosystem services provided in degraded, replanted, and mature mangroves

After normalizing the data, the mature mangrove exhibited the highest estimation (values close to or equal to 1) for providing ecosystem services related to regulation (i.e., contaminant immobilization and carbon sequestration) and support (i.e., nutrient cycling). Conversely, the degraded mangrove showed the lowest service estimates with normalized values of 0.2 for contaminant immobilization, 0.1 for carbon sequestration, and 0.7 for nutrient cycling, indicating a reduced capacity to provide the assessed regulation and support services. In the replanted mangroves, the results indicate a gradual effect in the provision of ecosystem services as the mangrove develops. The normalized estimates for contaminant immobilization were 0.5 and 0.8 in the 9- and 13-years-old replanted areas, respectively. For carbon sequestration, the values were 0.3 (9-years-old) and 0.5 (13-years-old), while for nutrient cycling, they were 0.8 (9-years-old) and 1.0 (13-years-old; Fig. 4).

Discussion

Edaphic features controlling soil quality and ecosystem functioning

Our findings indicate that mangrove replanting was effective in restoring soil parameter contents (Table 2) that string the soil quality and ecosystem's functioning for contaminant immobilization, carbon sequestration, and nutrient cycling (Fig. 2). These results corroborate a previous conducted in the same location which reported that mangrove development increased soil carbon and minerals present in fine particles (e.g., iron minerals), contributing to enhanced SCS and contaminant retention capacity². Indeed, the vector directions in the PCA revealed that variables such as FeEX, FeFR, FeLP, FeCR, FePY, DOP, pseudo-total Fe, SOC, clay, silt, available

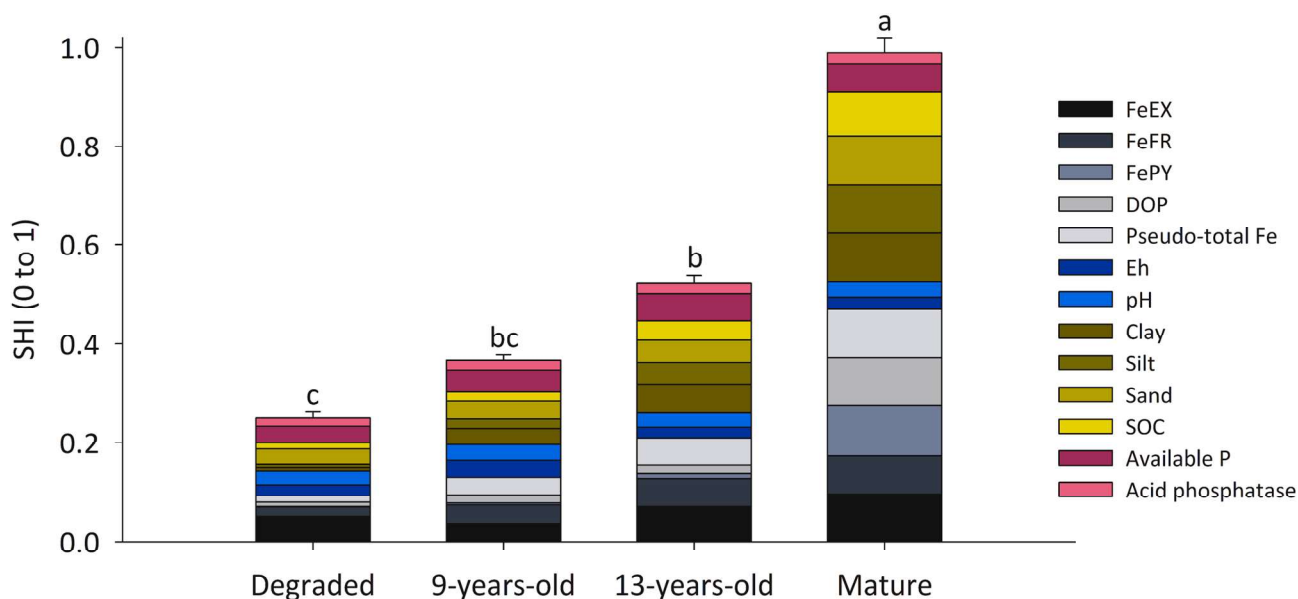


Fig. 3. Soil quality index (SHI) results for degraded, 9-years-old replanted, 13-years-old replanted, and mature mangrove areas. The bars represent the sum of individual SHI values for each selected variable. The differences between SHI values for each studied area were assessed using the Kruskal-Wallis followed by Dunn's post-hoc comparison at $p < 0.05$. FeEX: exchangeable iron; FeFR: ferrihydrite-associated iron; FePY: pyritic iron; DOP: degree of iron pyritization; SOC: soil organic carbon; Eh: redox potential.

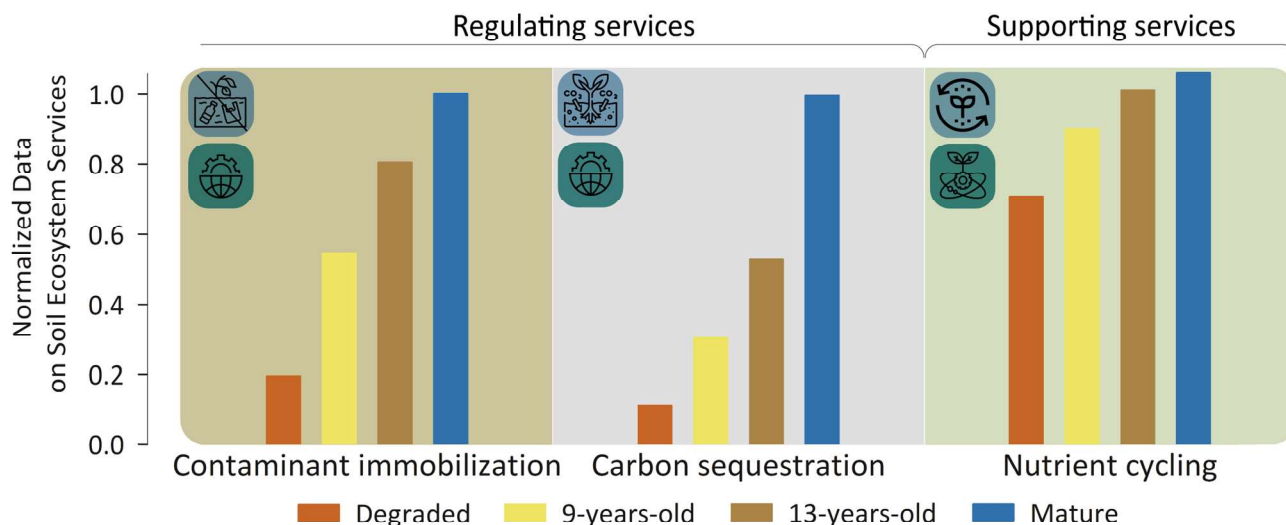


Fig. 4. Illustrative scheme of the estimation of regulating and supporting ecosystem services provided by mangroves in different scenarios (i.e., degradation, replanted, and mature conditions). The bars represent normalized data from the following soil variables: FeFR (ferrihydrite-associated iron), FeLP (lepidocrocite-associated iron), FeCR (hematite and goethite-associated iron), and FePY (pyritic iron) contents for contaminant immobilization; SOC (soil organic carbon), pseudo-total Fe, and clay contents for carbon sequestration; and available P, and the activity of enzymes acid phosphatase and β -glucosidase for nutrient cycling.

P, acid phosphatase, and β -glucosidase exerted a greater influence on mature mangrove soil, with replanted mangroves gradually being affected by these variables compared to degraded mangroves (Fig. 2).

In mangrove soils subject to redox variation and prevailing suboxic conditions, as observed in this study (Table 2), the coupled C-Fe dynamics plays a key role in carbon sequestration and contaminant immobilization^{67,68}. Under suboxic conditions, iron reduction (present in iron oxyhydroxides) and sulfate reduction mediated by anaerobic bacteria are the primary pathways of soil organic decomposition^{6,69,70}. These low decomposition rate pathways favor the soil carbon accumulation from vegetation⁷¹⁻⁷³. Additionally, the end product of iron and

sulfate reduction reactions is the formation of pyrite, which can co-precipitate with heavy metals, promoting contaminants retention^{26,74,75}. Indeed, the contents of FeFR, FeLP, FeCR, FePY, pseudo-total Fe, SOC, and SCS were significantly higher in replanted mangroves compared to degraded (Table 2) enhancing the soil quality (Fig. 3) associated with capacity to carbon storage and contaminants retention.

Additionally, the contents of available P and the activity of the enzymes β -glucosidase and acid phosphatase were significantly higher in replanted mangroves compared to degraded (Table 2) reflecting in a higher soil quality (Fig. 3) associated with nutrient cycling. These results point out the role of vegetation in providing available P⁷⁶ and the increased microbial activity influencing nutrient availability^{77,78} in replanted mangrove soils. It is noteworthy that in the degraded area (no vegetation), phosphorus input may come from anthropogenic sources surrounding the study area², and lower acid phosphatase activity implies that phosphorus in the soil is more solubilized and bioavailable⁷⁹ and may be exported to adjacent mangroves^{80,81}. On the other hand, that higher values of acid phosphatase indicate that, despite being present in higher contents, phosphorus is less bioavailable to plants and is retained in the soil mineral fractions^{82–84}. Furthermore, the higher activity of the enzyme β -glucosidase in replanted mangroves, similar to mature mangroves, indicates the restoration of microbial activity involved in soil organic matter decomposition and, ultimately, nutrient mineralization in the soil^{85–87}.

In this context, as the mangrove develops the restoration of ecosystem functions associated with specific soil variables is reflected in the SHI (Fig. 3) formulated by PCA (Fig. 2). Mangrove soils exhibit unique characteristics influenced by factors such as redox potential, tidal influence, vegetation composition, fauna activity, and mineral composition. By selecting specific variables that capture these features, the SHI is formulated to the distinctive nature of scenarios and promote a more effective understanding of the functioning of the ecosystem^{41,88}. Previous studies emphasize the importance of considering various components, including those related to the mangrove forest, soil, surrounding marine ecosystem, hydrology, and socio-economic factors, to formulate a comprehensive quality index^{3,89–91}.

Soil health index as a feasible tool for assessing mangrove status and provision of ecosystem services

In mangrove ecosystems, SHI may be a tool for transmitting knowledge in a viable way and to help assess the impact of human activities, guide sustainable resource use, and plan conservation strategies^{2,92,93}. Accordingly, the SHI contributes to conveying complex information to a broader audience (e.g., decision-makers and communities whose livelihoods depend on the mangrove forests)^{36,94}. Indeed, previous studies have reported that simplifying scientific data into quality indexes facilitates effective communication and collaboration among stakeholders^{92,95,96}. Our findings reveal that monitoring specific variables related to ecosystem services (e.g., carbon sequestration, nutrient cycling) and formulating an SHI provides a scientific foundation for implementing regulations and initiatives that support ecosystem health, its conservation, and restoration initiatives.

The formulation of quality indexes has been applied on different frontiers. For instance, in Brazil, Alkalay et al.⁹⁷ developed a clean-coast index to measure plastic debris as a beach cleanliness indicator which the authors suggest as a tool for the “Clean Coast” program—a new, long-term approach to cleaner beaches and facilitating an increase in public awareness. Duarte et al.⁹⁸ aimed to develop a multi-level biological index for diagnosing threats to mangrove areas which may be an effective tool for evaluating mangrove conservation statuses and encourage environmental institutions to prioritize adequate actions.

In our study, the SHI in the different scenarios investigated (Fig. 3) reflects the provision of ecosystem services related to regulation (i.e., contaminant immobilization and carbon sequestration) and support (i.e., nutrient cycling; Fig. 4) based on variables governing the geochemical functioning of mangroves (Fig. 2). The ecosystem services provided by mangrove forests vary spatially and thus can influence where to prioritize mangrove protection and restoration that can help bolster local benefits communities while promoting carbon sequestration to meet climate goals⁹⁹. However, previous studies report that in many communities, the perception of regulation and support services (e.g., nutrient cycling) is less evident compared to provisioning services^{100,101}. Afonso et al.¹⁰² reported that mangrove ecosystems as perceived by the local communities can guide conservation efforts by targeting specific threats such as over-exploitation, pollution, or habitat degradation. Moreover, the more inclusive decision-making processes concerning conservation and reforestation planning of mangrove forests may be better targeted when ecosystem services are recognized and estimated^{103,104}.

This study provides an initial framework for assessing soil health in mangrove ecosystems; however, some limitations should be acknowledged. The SHI proposed here is based on a single temporal sampling, which constrains its ability to capture short-term fluctuations in soil properties driven by tidal dynamics^{105–107} and seasonal rainfall⁵². Future studies should include temporal monitoring adjusted to local climatic conditions to strengthen SHI as a long-term tool for ecosystem assessment. Moreover, geoenvironmental factors such as land use, geology, and climate must be considered in large-scale applications to ensure that SHI comparisons are made among environmentally compatible sites⁷. Integrating SHI into predictive models such as InVEST^{108,109} could further enhance its capacity to forecast changes in ecosystem services under different restoration or management scenarios. In Brazil, the implementation of SHI-based assessments could support national blue carbon initiatives and mangrove restoration programs by offering a soil-based metric of functional recovery.

Conclusions

We developed a mangrove-specific Soil Health Index (SHI) that integrates redox-sensitive, biological, and physical–chemical attributes into a single operational metric. The SHI distinguished contrasting site conditions and tracked recovery in restored stands, with mature mangroves operating near full capacity (0.99 ± 0.03), degraded sites at only a quarter of that capacity (0.25 ± 0.01), and replanted stands showing progressive recovery from 0.37 ± 0.01 after 9 years to 0.52 ± 0.02 after 13 years. These results demonstrate the sensitivity of SHI to

capture restoration trajectories and their implications for ecosystem services such as carbon sequestration, contaminant retention, and nutrient cycling.

By integrating key indicators of soil functioning, SHI provides a compact and reproducible way to summarize ecosystem health that is directly relevant to both science and management. While future calibration across different hydro-geomorphic contexts will be necessary to test its robustness, the index already offers a transparent measure that complements vegetation-based assessments. Beyond its technical merits, SHI represents a valuable communication tool, translating complex scientific data into accessible information that can support decision-making, foster collaboration among stakeholders, and guide conservation and reforestation strategies. In this sense, SHI contributes not only to advancing scientific understanding of mangrove soils but also to strengthening the link between ecological processes, ecosystem services, and societal benefits.

Data availability

The datasets generated and/or analyzed during the current study are available from the corresponding author on reasonable request.

Received: 3 September 2025; Accepted: 27 November 2025

Published online: 10 December 2025

References

- Lehmann, J., Bossio, D. A., Kögel-Knabner, I. & Rillig, M. C. The concept and future prospects of soil health. *Nat. Rev. Earth Environ.* **1**, 544–553 (2020).
- Jimenez, L. C. Z., Queiroz, H. M., Cherubin, M. R. & Ferreira, T. O. Applying the soil management assessment framework (SMAF) to assess Mangrove soil quality. *Sustainability* **14**, 3085 (2022).
- Tripathi, R. et al. Soil quality in Mangrove ecosystem deteriorates due to rice cultivation. *Ecol. Eng.* **90**, 163–169 (2016).
- Jimenez, L. C. Z. et al. Recovery of soil processes in replanted mangroves: implications for soil functions. *Forests* **13**, 422 (2022).
- Ferreira, T. O. et al. Litho-climatic characteristics and its control over Mangrove soil geochemistry: A macro-scale approach. *Sci. Total Environ.* **811**, 152152 (2022).
- Alongi, D. M. 85–103. <https://doi.org/10.1029/CE060p0085> (2005).
- Mello, F. A. O. et al. Soil health and ecosystem services in mangrove forests: A global overview. *Water (Switzerland)* **16**, (2024).
- Sharma, S., Jain, P. K. & Soloman, P. E. Carbon storage potential of soil in diverse terrestrial ecosystems. *Nat. Environ. Pollut Technol.* **22**, 1809–1819 (2023).
- Mandal, U. K. et al. 161–188. <https://doi.org/10.1002/9780891187400.ch6> (2025).
- Kumar, U., Kaviraj, M., Panneerselvam, P. & Nayak, A. K. Conversion of mangroves into rice cultivation alters functional soil microbial community in sub-humid tropical paddy soil. *Front. Environ. Sci.* **10**, (2022).
- Panda, S. K. & Das, S. Potential of plant growth-promoting microbes for improving plant and soil health for biotic and abiotic stress management in Mangrove vegetation. *Rev. Environ. Sci. Bio/Technology.* **23**, 801–837 (2024).
- Macreadie, P. I. et al. Blue carbon as a natural climate solution. *Nat. Rev. Earth Environ.* **2**, 826–839 (2021).
- Alongi, D. M. Carbon cycling and storage in Mangrove forests. *Annu. Rev. Mar. Sci.* **6**, 195–219 (2014).
- Chausson, A. et al. Mapping the effectiveness of nature-based solutions for climate change adaptation. *Glob Chang. Biol.* **26**, 6134–6155 (2020).
- Seddon, N. et al. Understanding the value and limits of nature-based solutions to climate change and other global challenges. *Philos. Trans. R Soc. B Biol. Sci.* **375**, 20190120 (2020).
- McLeod, E. et al. A blueprint for blue carbon: toward an improved Understanding of the role of vegetated coastal habitats in sequestering CO₂. *Front. Ecol. Environ.* **9**, 552–560 (2011).
- Twilley, R. R., Rovai, A. S. & Riul, P. Coastal morphology explains global blue carbon distributions. *Front. Ecol. Environ.* **16**, 503–508 (2018).
- Ruiz, F. et al. Iron's role in soil organic carbon (de)stabilization in mangroves under land use change. *Nat. Commun.* **15**, 10433 (2024).
- Kim, J. et al. Microbial decomposition of soil organic matter determined by edaphic characteristics of Mangrove forests in East Asia. *Sci. Total Environ.* **763**, 142972 (2021).
- Nóbrega, G. N. et al. Edaphic factors controlling summer (rainy season) greenhouse gas emissions (CO₂ and CH₄) from semiarid Mangrove soils (NE-Brazil). *Sci. Total Environ.* **542**, 685–693 (2016).
- Alongi, D. M. et al. Sediment accumulation and organic material flux in a managed Mangrove ecosystem: estimates of land-ocean-atmosphere exchange in Peninsular Malaysia. *Mar. Geol.* <https://doi.org/10.1016/j.margeo.2004.04.016> (2004).
- Friesen, S. D., Dunn, C. & Freeman, C. Decomposition as a regulator of carbon accretion in mangroves: a review. *Ecol. Eng.* **114**, 173–178 (2018).
- Nóbrega, G. N., Ferreira, T. O., Romero, R. E., Marques, A. G. B. & Otero, X. L. Iron and sulfur geochemistry in semi-arid Mangrove soils (Ceará, Brazil) in relation to seasonal changes and shrimp farming effluents. *Environ. Monit. Assess.* **185**, 7393–7407 (2013).
- Alongi, D. M. Carbon cycling in the world's Mangrove ecosystems revisited: significance of Non-Steady state diagenesis and subsurface linkages between the forest floor and the coastal ocean. *Forests* **11**, 977 (2020).
- Howard, J. et al. Coastal blue carbon: methods for assessing carbon stocks and emissions factors in mangroves, tidal salt marshes, and seagrasses. *Conserv. Int.* **1** (Conservation International, Intergovernmental Oceanographic Commission of UNESCO, International Union for Conservation of Nature, 2014).
- Machado, W. et al. Trace metal pyritization variability in response to Mangrove soil aerobic and anaerobic oxidation processes. *Mar. Pollut Bull.* **79**, 365–370 (2014).
- Marchand, C. et al. Heavy metals distribution in Mangrove sediments along the mobile coastline of French Guiana. *Mar. Chem.* **98**, 1–17 (2006).
- Queiroz, H. M., Nóbrega, G. N., Otero, X. L. & Ferreira, T. O. Are acid volatile sulfides (AVS) important trace metals sinks in semi-arid mangroves? *Mar. Pollut Bull.* **126**, 318–322 (2018).
- Duke, N. C. et al. A world without mangroves? *Science* **80**. <https://doi.org/10.1126/science.317.5834.41b> (2007).
- Polidoro, B. A. et al. The loss of species: Mangrove extinction risk and geographic areas of global concern. *PLoS One.* **5**, e10095 (2010).
- Ferreira, A. C. & Lacerda, L. D. Degradation and conservation of Brazilian mangroves, status and perspectives. *Ocean. Coast Manag.* **125**, 38–46 (2016).
- Godoy, M. D. P., De Andrade Meireles, A. J. & De Lacerda, L. D. Mangrove response to land use change in estuaries along the semiarid Coast of Ceará, Brazil. *J. Coast Res.* **34**, 524–533 (2018).

33. Lewis, R. R. & Gilmore, R. G. Important considerations to achieve successful Mangrove forest restoration with optimum fish habitat. *Bull. Mar. Sci.* **80**, 823–837 (2007).
34. West, A. Ecosystem services. *Proc. Natl. Acad. Sci.* **112**, 7337–7338 (2015).
35. Winterwerp, J. C. et al. Managing erosion of mangrove-mud Coasts with permeable dams – lessons learned. *Ecol. Eng.* **158**, 106078 (2020).
36. Marion, L. F. et al. Development of a soil quality index to evaluate agricultural cropping systems in Southern Brazil. *Soil. Tillage Res.* **218**, 105293 (2022).
37. Gatt, Y. M. et al. The Mangrove restoration tracker tool: meeting local practitioner needs and tracking progress toward global targets. *One Earth.* **7**, 2072–2085 (2024).
38. Okarda, B. et al. Bridging technology and local participation: A collaborative approach for peatland and Mangrove restoration. *IOP Conf. Ser. Earth Environ. Sci.* **1506**, 012010 (2025).
39. Pimple, U. et al. Tracking Mangrove ecosystem dynamics: A remote sensing approach for species classification and conservation assessment. *Glob Ecol. Conserv.* **63**, e03865 (2025).
40. Mohan, M. et al. Challenges and opportunities integrating remote sensing for Mangrove conservation in Papua new guinea's complex natural and human landscapes. *Reg. Stud. Mar. Sci.* **89**, 104361 (2025).
41. Faridah-Hanum, I. et al. Development of a comprehensive Mangrove quality index (MQI) in Matang Mangrove: assessing Mangrove ecosystem health. *Ecol. Indic.* **102**, 103–117 (2019).
42. de Moraes, J. O. et al. Caracterização Fisiográfica E Geoambiental Da Zona Costeira Do Estado Do Ceará. *Erosão Progradação Litoral Bras.* (2006).
43. Barros, E. L., de Paula, D. P., Guerra, R. G. P. & de Oliveira Santos, J. *Pract. Reg. Sci. Sustain. Reg. Dev.* 127–150. https://doi.org/10.1007/978-981-16-2221-2_6 (Springer Singapore, 2021).
44. Albuquerque, M. D. G., Calliari, L. J., Corrêa, I. C. S. & Pinheiro, L. D. S. Morfodinâmica Da Praia do Futuro, Fortaleza-CE: Uma Síntese de dois Anos de Estudo. *Quat Environ. Geosci.* **1**, 49–57 (2009).
45. Queiroz Pereira, A. 51–68. https://doi.org/10.1007/978-3-030-46593-3_4 (2020).
46. Otero, X. L. et al. High fragility of the soil organic C pools in Mangrove forests. *Mar. Pollut. Bull.* <https://doi.org/10.1016/j.marpollbul.2017.03.074> (2017).
47. Araújo Júnior, J. M. C. et al. Selective geochemistry of iron in Mangrove soils in a semiarid tropical climate: effects of the burrowing activity of the crabs *Ucides cordatus* and *Uca Maracoani*. *Geo-Mar. Lett.* **32**, 289–300 (2012).
48. Otero, X. L. et al. Crab bioturbation and seasonality control nitrous oxide emissions in semiarid Mangrove forests (Ceará, Brazil). *Appl. Sci.* **10**, (2020).
49. Tessier, A., Campbell, P. G. C. & Bisson, M. Sequential extraction procedure for the speciation of particulate trace metals. *Anal. Chem.* **51**, 844–851 (1979).
50. Huerta-Diaz, M. A. & Morse, J. W. A quantitative method for determination of trace metal concentrations in sedimentary pyrite. *Mar. Chem.* **29**, 119–144 (1990).
51. Fortin, D., Leppard, G. G. & Tessier, A. Characteristics of lacustrine diagenetic iron oxyhydroxides. *Geochim. Cosmochim. Acta.* **57**, 4391–4404 (1993).
52. Ferreira, T. O. et al. Windsock behavior: Climatic control on iron biogeochemistry in tropical mangroves. *Biogeochemistry* **156**, 437–452 (2021).
53. Berner, R. A. Sedimentary pyrite formation. *Am. J. Sci.* **268**, 1–23 (1970).
54. Klute, A., Gee, G. W. & Bauder, J. W. *Methods Soil Anal. Part 1—Physical Mineral. Methods* **3**, 383–411. (Soil Science Society of America, American Society of Agronomy, 1986).
55. Mehlich. *Short Test Methods Used Soil Test. Div. Dep. Agric. Raleigh, North Carolina* 1–53 (University of North Carolina, 1953).
56. Tabatabai, M. A. & Bremner, J. M. Use of p-nitrophenyl phosphate for assay of soil phosphatase activity. *Soil. Biol. Biochem.* **1**, 301–307 (1969).
57. Eivazi, F. & Tabatabai, M. A. Glucosidases and galactosidases in soils. *Soil. Biol. Biochem.* **20**, 601–606 (1988).
58. Brejda, J. J., Moorman, T. B., Karlen, D. L. & Dao, T. H. Identification of regional soil quality factors and indicators I. Central and Southern high plains. *Soil. Sci. Soc. Am. J.* **64**, 2115–2124 (2000).
59. Mukhopadhyay, S. et al. Soil quality index for evaluation of reclaimed coal mine spoil. *Sci. Total Environ.* **542**, 540–550 (2016).
60. Karlen, D. L. et al. Soil quality: A Concept, Definition, and framework for evaluation (A guest Editorial). *Soil. Sci. Soc. Am. J.* **61**, 4–10 (1997).
61. Beauducel, A. & Spohn, F. Retained-Components factor transformation: factor loadings and factor score predictors in the column space of retained components. *J. Mod. Appl. Stat. Methods.* **13**, 106–130 (2014).
62. Bieluczyk, W. et al. Forest restoration rehabilitates soil multifunctionality in riparian zones of sugarcane production landscapes. *Sci. Total Environ.* **888**, 164175 (2023).
63. Liebig, M. A., Varvel, G. & Doran, J. A. Simple Performance-Based index for assessing multiple agroecosystem functions. *Agron. J.* **93**, 313–318 (2001).
64. Bhardwaj, A. K., Jasrotia, P., Hamilton, S. K. & Robertson, G. P. Ecological management of intensively cropped agro-ecosystems improves soil quality with sustained productivity. *Agric. Ecosyst. Environ.* **140**, 419–429 (2011).
65. Thanh-Nho, N., Marchand, C., Strady, E., Vinh, T. V. & Nhu-Trang, T. T. Metals geochemistry and ecological risk assessment in a tropical Mangrove (Can Gio, Vietnam). *Chemosphere* **219**, 365–382 (2019).
66. Queiroz, H. M. et al. Changes in soil iron biogeochemistry in response to Mangrove dieback. *Biogeochemistry* **158**, 357–372 (2022).
67. Dícen, G. P., Navarrete, I. A., Rallos, R. V., Salmo, S. G. & Garcia, M. C. A. The role of reactive iron in long-term carbon sequestration in Mangrove sediments. *J. Soils Sediments.* **19**, 501–510 (2019).
68. Otero, X. L. & Macías, F. *Biogeochemistry and Pedogenetic Process in Saltmarsh and Mangrove Systems* (Nova Science Publishers, 2010).
69. Canfield, D. E., Thamdrup, B. & Hansen, J. W. The anaerobic degradation of organic matter in Danish coastal sediments: iron reduction, manganese reduction, and sulfate reduction. *Geochim. Cosmochim. Acta.* **57**, 3867–3883 (1993).
70. Holmer, M. et al. Biogeochemical cycling of sulfur and iron in sediments of a south-east Asian mangrove, Phuket Island, Thailand. *Biogeochemistry* **26**, (1994).
71. Kristensen, E., Bouillon, S., Dittmar, T. & Marchand, C. Organic carbon dynamics in Mangrove ecosystems: A review. *Aquat. Bot.* **89**, 201–219 (2008).
72. Ferreira, T. O., Vidal-Torrado, P., Otero, X. L. & Macías, F. Are Mangrove forest substrates sediments or soils? A case study in southeastern Brazil. *CATENA* **70**, 79–91 (2007).
73. Vidal-Torrado, P. et al. *Biogeochem Pedogenetic Process. Saltmarsh Mangrove Syst.* 27–56 (2010).
74. Matagi, S., Swai, D. & Mugabe, R. A review of heavy metal removal mechanisms in wetlands. *African J. Trop. Hydrobiol. Fish* **8**, (1998).
75. Marchand, C., Lallier-Vergès, E. & Allenbach, M. Redox conditions and heavy metals distribution in Mangrove forests receiving effluents from shrimp farms (Teremba Bay, new Caledonia). *J. Soils Sediments.* **11**, 529–541 (2011).
76. Boto, K. G. *Pollut. Trop. Aquat. Syst.* 129–145 (CRC Press, 2018).
77. Alongi, D. Impact of global change on nutrient dynamics in Mangrove forests. *Forests* **9**, 596 (2018).

78. Dinesh, R., Ghoshal & Chaudhuri Soil biochemical/microbial indices as ecological indicators of land use change in Mangrove forests. *Ecol. Indic.* **32**, 253–258 (2013).
79. Behera, B. C. et al. Phosphate solubilization and acid phosphatase activity of *Serratia* sp. isolated from Mangrove soil of Mahanadi river delta, Odisha, India. *J. Genet. Eng. Biotechnol.* **15**, 169–178 (2017).
80. Adame, M. F. & Lovelock, C. E. Carbon and nutrient exchange of Mangrove forests with the coastal ocean. *Hydrobiologia* **663**, 23–50 (2011).
81. Singh, G., Chauhan, R., Ranjan, R. K., Prasad, M. B. & Ramanathan, A. L. Phosphorus dynamics in mangroves of India. *Curr. Sci.* 1874–1881 (2015).
82. Oberson, A., Besson, J. M., Maire, N. & Sticher, H. Microbiological processes in soil organic phosphorus transformations in conventional and biological cropping systems. *Biol. Fertil. Soils.* **21**, 138–148 (1996).
83. Rejsek, K., Vranova, V. & Formanek, P. Determination of the proportion of total soil extracellular acid phosphomonoesterase (E.C. 3.1.3.2) activity represented by roots in the soil of different forest ecosystems. *Sci. World J.* **2012**. (2012).
84. Cardoso, E. J. B. N. & Andreote, F. D. *Microbiologia Do Solo* <https://doi.org/10.11606/9788586481567> (Universidade de São Paulo. Escola Superior de Agricultura Luiz de Queiroz, 2020).
85. Liu, H., Tian, Y., Zheng, T., Yan, C. & Hong, H. Studies of glucosidase activities from surface sediments in Mangrove swamp. *J. Exp. Mar. Bio Ecol.* **367**, 111–117 (2008).
86. Ekenler, M. β -Glucosaminidase activity of soils: effect of cropping systems and its relationship to nitrogen mineralization. *Biol. Fertil. Soils.* **36**, 367–376 (2002).
87. Adetunji, A. T., Lewu, F. B., Mulidzi, R. & Ncube, B. The biological activities of β -glucosidase, phosphatase and urease as soil quality indicators: a review. *J. soil. Sci. plant. Nutr.* **17**, 794–807 (2017).
88. Ibrahim, F. H. et al. How to develop a comprehensive mangrove quality index? *MethodsX* **6**, 1591–1599 (2019).
89. Mohamad Pazi, A. M., Khan, W. R., Nuruddin, A. A., Adam, M. B. & Gandaseca, S. Development of mangrove sediment quality index in Matang mangrove forest reserve, Malaysia: a synergetic approach. *Forests* **12**, 1279 (2021).
90. Gunathilaka, M. D. K. L. & Harhana, W. T. S. The implementation of the Mangrove quality index: A way to overcome overestimation and classification concerns in detecting Mangrove forest cover. *Int. J. Environ. Eng. Educ.* **5**, 1–8 (2023).
91. Mustapha, A., Gandaseca, S., Hanafi, A. & Nurhidayu, S. Sediment quality index in Mangrove forest. *Pertanika J. Sch. Res. Rev.* **3**, 41–51 (2017).
92. De Laurentiis, V. et al. Soil quality index: exploring options for a comprehensive assessment of land use impacts in LCA. *J. Clean. Prod.* **215**, 63–74 (2019).
93. Lal, R. Restoring soil quality to mitigate soil degradation. *Sustainability* **7**, 5875–5895 (2015).
94. Blecker, S. W., Stillings, L. L., Amacher, M. C., Ippolito, J. A. & DeCrappeo, N. M. Development and application of a soil organic matter-based soil quality index in mineralized terrane of the Western US. *Environ. Earth Sci.* **68**, 1887–1901 (2013).
95. Ives, Z. G. 1–4. https://doi.org/10.1007/978-3-642-02879-3_1 (2009).
96. Cooper, J. A. G., Ramm, A. E. L. & Harrison, T. D. The estuarine health index: A new approach to scientific information transfer. *Ocean. Coast Manag.* **25**, 103–141 (1994).
97. Alkalay, R., Pasternak, G. & Zask, A. Clean-coast index—A new approach for beach cleanliness assessment. *Ocean. Coast Manag.* **50**, 352–362 (2007).
98. Duarte, L. F., de Souza, A., de Nobre, C. A., Pereira, C. R., Pinheiro, M. A. A. & C. D. S. & Multi-level biological responses in *Ucides cordatus* (Linnaeus, 1763) (Brachyura, Ucididae) as indicators of conservation status in Mangrove areas from the Western Atlantic. *Ecotoxicol. Environ. Saf.* **133**, 176–187 (2016).
99. Arkema, K. K. et al. Evidence-based target setting informs blue carbon strategies for nationally determined contributions. *Nat. Ecol. Evol.* **7**, 1045–1059 (2023).
100. Su, J. & Gasparatos, A. Perceptions about Mangrove restoration and ecosystem services to inform ecosystem-based restoration in large Xiamen Bay, China. *Landsc. Urban Plan.* **235**, 104763 (2023).
101. Nyangoko, B. P., Berg, H., Mangora, M. M., Shalli, M. S. & Gullström, M. Local perceptions of changes in Mangrove ecosystem services and their implications for livelihoods and management in the Rufiji Delta, Tanzania. *Ocean. Coast Manag.* **219**, 106065 (2022).
102. Afonso, F. et al. Community perceptions about Mangrove ecosystem services and threats. *Reg. Stud. Mar. Sci.* **49**, 102114 (2022).
103. Reyes-Arroyo, N., Camacho-Valdez, V. & Saenz-Arroyo, A. Infante-Mata, D. Socio-cultural analysis of ecosystem services provided by mangroves in La encrucijada biosphere Reserve, southeastern Mexico. *Local. Environ.* **26**, 86–109 (2021).
104. Ruslan, N. F. N., Goh, H. C., Hattam, C., Edwards-Jones, A. & Moh, H. H. Mangrove ecosystem services: contribution to the well-being of the coastal communities in Klang Islands. *Mar. Policy.* **144**, 105222 (2022).
105. Knight, J. M., Griffin, L., Dale, P. E. R. & Sheaves, M. Short-term dissolved oxygen patterns in sub-tropical mangroves. *Estuar. Coast Shelf Sci.* **131**, 290–296 (2013).
106. Pérez, A., Gutiérrez, D., Saldarriaga, M. S. & Sanders, C. J. Tidally driven sulfidic conditions in Peruvian Mangrove sediments. *Geo-Mar. Lett.* **38**, 457–465 (2018).
107. Romigh, M. M., Davis, S. E., Rivera-Monroy, V. H. & Twilley, R. R. Flux of organic carbon in a riverine Mangrove wetland in the Florida coastal everglades. *Hydrobiologia* **569**, 505–516 (2006).
108. Rosa, L. N., de Paula Costa, D., de Freitas, D. M. & M. & Modelling spatial-temporal changes in carbon sequestration by mangroves in an urban coastal landscape. *Estuar. Coast Shelf Sci.* **276**, 108031 (2022).
109. de Andrade, C. H., Duarte de Paula Costa, M. & de Freitas, D. M. Assessing the carbon sequestration potential by mangroves in a coastal metropolitan region. *Reg. Stud. Mar. Sci.* **90**, 104478 (2025).

Acknowledgements

We thank the Center for Carbon Research in Tropical Agriculture (CCARBON) for providing infrastructure support. We are also grateful to CAPES, CNPq, and FAPESP for their institutional support, which enabled the execution of this research.

Author contributions

LCZJ, Conceptualization, Formal analysis, Investigation, Writing—Original Draft, and Writing—Review & Editing. HMQ, Conceptualization, Data Curation, Funding acquisition, Writing—Original Draft, and Writing - Review & Editing. MRC, Conceptualization, Resources, Writing—Original Draft, and Writing—Review & Editing. FR, Data Curation, Writing—Original Draft, and Writing—Review & Editing. TOF, Conceptualization, Supervision, Funding acquisition, Investigation, Writing—Original Draft, and Writing—Review & Editing.

Funding

This work received financial support provided by the National Council for Scientific and Technological Development (CNPq, grants number 305013/2022-0, 440024/2024-2 to TOF, 302249/2025-7 to MRC, and 307707/2025-

3 to HMQ), Coordination of Superior Level Staff Improvement (CAPES, Finance Code 001), São Paulo Research Foundation (FAPESP, grants number and 2022/08732-0 to LCZJ and 2024/18195-7 to HMQ) and USP Process n. 22.1.09345.01.2 (University of São Paulo, project number 10, Notice Program for Support to New Faculty Members 2024/1). We gratefully acknowledge the support of the RCGI – Research Centre for Greenhouse Gas Innovation (23.1.8493.1.9), hosted by the University of São Paulo (USP) and sponsored by FAPESP – São Paulo Research Foundation (2020/15230-5), and sponsored by PETRONAS Petróleo Brasil Ltda, and the strategic importance of the support given by ANP (Brazil's National Oil, Natural Gas and Biofuels Agency) through the R&DI levy regulation (ANP – Project #23.702-4; BlueShore).

Declarations

Competing interests

The authors declare no competing interests.

Additional information

Supplementary Information The online version contains supplementary material available at <https://doi.org/10.1038/s41598-025-30909-2>.

Correspondence and requests for materials should be addressed to H.M.Q. or T.O.F.

Reprints and permissions information is available at www.nature.com/reprints.

Publisher's note Springer Nature remains neutral with regard to jurisdictional claims in published maps and institutional affiliations.

Open Access This article is licensed under a Creative Commons Attribution-NonCommercial-NoDerivatives 4.0 International License, which permits any non-commercial use, sharing, distribution and reproduction in any medium or format, as long as you give appropriate credit to the original author(s) and the source, provide a link to the Creative Commons licence, and indicate if you modified the licensed material. You do not have permission under this licence to share adapted material derived from this article or parts of it. The images or other third party material in this article are included in the article's Creative Commons licence, unless indicated otherwise in a credit line to the material. If material is not included in the article's Creative Commons licence and your intended use is not permitted by statutory regulation or exceeds the permitted use, you will need to obtain permission directly from the copyright holder. To view a copy of this licence, visit <http://creativecommons.org/licenses/by-nc-nd/4.0/>.

© The Author(s) 2025